Mineralogical properties of the caprock and reservoir sandstone of the Heletz field scale experimental CO2 injection site, Israel; and their initial sensitivity to CO2 injection.

Mineralogical properties of the caprock and reservoir sandstone of the Heletz field scale experimental CO_2 injection site, Israel; and their initial sensitivity to CO_2 injection.

Edlmann K.[1], Niemi A. [2], Bensabat J. [3], Haszeldine R.S. [1] and McDermott C.I. [1]

[1]School of GeoSciences, University of Edinburgh, Grant Institute, The King's Buildings, University of Edinburgh, James Hutton Road, Edinburgh, EH9 3FE. United Kingdom.
[2]Uppsala University, Department of Earth Sciences, Villavägen 16, SE-75236 Uppsala, Sweden.
[3]EWRE, Haifa, Israel.

Corresponding Author

Katriona Edlmann: School of Geoscience, Grant Institute, The King's Buildings, University of Edinburgh, James Hutton Road, Edinburgh, EH9 3FE United Kingdom.

kedlmann@staffmail.ed.ac.uk

Telephone: +44 (0) 131-650-7339

Fax: +44 (0) 131-668-3184

1 Introduction

Concentrations of atmospheric CO_2 have increased by more than 35% since industrialisation began, UK Met Office (2010). To reduce the amount of CO_2 entering the Earth's atmosphere from increasing energy demands, Carbon Capture and Storage is being considered. CO_2 is separated from industrial emissions and injected in its supercritical phase into suitable deep geological formations. CO_2 saturated fluids and separated phase CO_2 are held in porous rocks sealed by overlying impermeable caprocks, Koide at al., (1992). The impermeable caprocks tend to be argillaceous mudstones, clays and shales which have a high sealing capacity due to their high capillary entry pressures, low permeability, high sorption capacity, high ion exchange capacity and potential swelling ability, IEAGHG, (2011). As $scCO_2$ is less dense and viscous than the saline formation fluids in the reservoir rock the injected CO_2 will experience an upwards buoyant force and migrate to accumulate against the underside of the impermeable caprock. Understanding the long term integrity of these caprock seals is a pre-requisite for CO_2 storage, DePaolo (2013), Bachu (2003), Busch et al. (2010), Li et al. (2005 & 2006), Class (2009), Ketzer et al. (2009), Fischer et al. (2010), Gaus (2010) and Amann et al. (2011).

During geological storage CO_2 is injected into the reservoir in its supercritical state (above 31.1°C and 7.3MPa or an 800m depth equivalent). CO_2 in its supercritical phase is lighter and less viscous that the formation brine making it more buoyant and mobile than the formation brine, even after injection has stopped, the CO_2 plume will continue to migrate in response to buoyancy and regional groundwater flow, Gaus (2010), Knauss et al. (2005). The collection of a reactive fluid like CO_2 saturate brine under the caprock and within the storage reservoir will result in chemical disequilibria and has the potential to initiate complex chemical dissolution and precipitation reactions within the caprock and reservoir rock minerals that may impact on the injectivity or the storage reservoir and security of the caprock integrity, Rochelle et al. (2004). A number of different CO_2 / formation brine / rock interactions are encountered as the plume migrates upwards towards the caprock, Kampman et al (2014), Fitts and Peters (2013), Michael et al (2010), Gaus (2010) and Griffith et al. (2011), Figure 1.

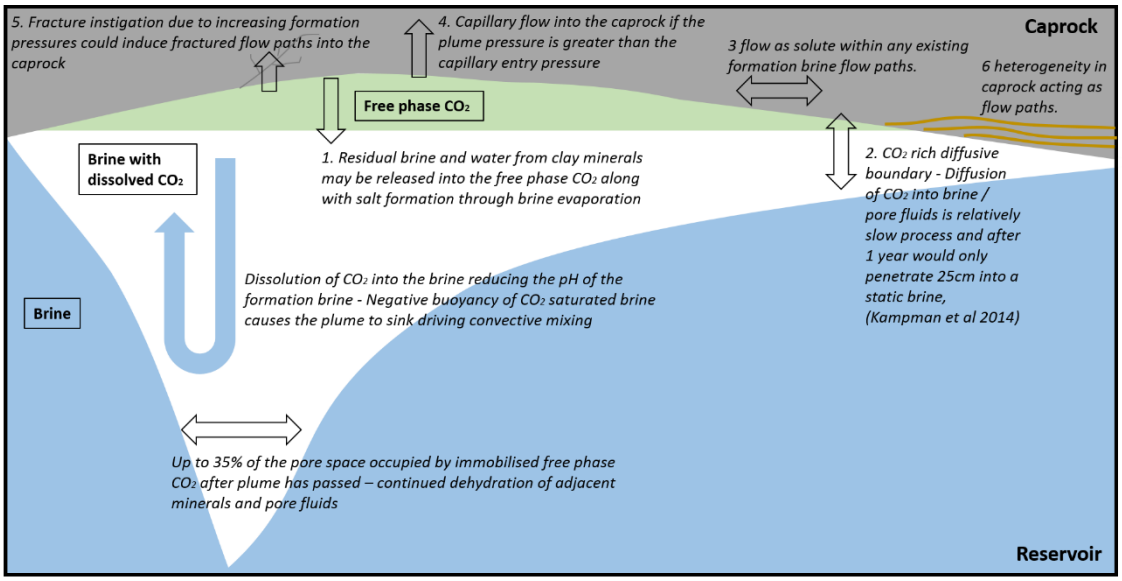

Figure 1 Cartoon of the primary CO_2 / brine / caprock contacts and interactions

At the leading edge of the CO_2 plume, the CO_2 will displace the formation brine in a drainage process and some CO_2 will dissolve into the formation brine, Duan and Sun (2003), Duan et al., (2006). When CO_2 gas dissolves in water, it lowers the pH of the formation fluid, through the production of carbonic acid (H_2CO_3), and its subsequent dissociation to bicarbonate (HCO_3^-) and carbonate (CO_3^{2-}), which releases protons (H^+), through the following reaction:

$$CO_2(aq) + H_2O \rightleftharpoons HCO_3^- + H^+ \rightleftharpoons CO_3^{2-} + 2H^+ \quad (1)$$

This lowered pH may enhance the dissolution of minerals; altering permeability or causing potential breakdown of the rock (or cement) matrix, Czernichowski-Lauriol et al. (2006) and Bensen et al. (2005). The rate and extent of mineral dissolution is dependent on the chemical composition of the fluid, the mineralogy of the rock, pressure, temperature and the kinetics of reaction, DePaolo (2013), which is in turn dependant on the reactive surface area, Landrot et al. (2012) and the mechanisms of dissolution. In general CO_2-acidified brines cause the dissolution of carbonate minerals (with relatively fast reaction rates, reaching equilibrium within a few hours, Rosenbauer et al. (2005)), and silicate minerals, in particular alumina-silicate minerals such as clays and feldspars, (with slow reaction rates of up to several thousands of years, Rosenqvist et al., (2014)). The presence of CO_2 can also lead to the dehydration of salts and clays leading to the shrinkage of clay minerals through the loss of interlayer water, Loring et al., (2013). If these reactions occur in the Heletz storage caprocks, the associated permeability and porosity changes may decrease the integrity of the caprock and reduce the security of CO_2 storage, Nogues et al (2013). If they occur within the reservoir storage rock, they may change the porosity, permeability and mechanical integrity of the reservoir leading to a change in the injectivity or induce wellbore collapse or sanding.

This paper presents an overview of the geological setting of the Heletz site and its depositional history, and the first mineralogy results from nine Heletz caprock and reservoir sandstone samples from Heletz wells H-2 and H-18, obtained through X-Ray Diffraction (XRD). It also presents the results from limited "cook and look" bench experiments that were conducted on the Heletz caprock and reservoir sandstone samples to identify if there was any immediate mineral reactivity within the caprock or reservoir sandstone on exposure to CO_2 that would change the permeability and cause concerns during well completion and initial injection of CO_2 at Heletz. This was achieved by exposing caprock and reservoir rock chips to CO_2 saturated brine under in-situ reservoir temperature and salinity in a reaction vessel and testing for any changes in mineralogy that are products of dissolution such as decreases in carbonates, alumiosilicates or kaolinite or an increase in illite over and above that of the rocks natural variability.

1.1 Heletz geological setting

The Heletz site is located in the Southern Mediterranean Coastal Plain of Israel and is currently a test site for the EU FP7 MUSTANG pilot injection experiment, where CO_2 injection under realistic storage site conditions provides important evidence of the processes which will influence the storage behaviour and caprock integrity, Niemi et al. (2012). The Heletz structure is an anticline fold with a crest of about 2 km by 4 km and a vertical closure of 70 m, Shtivelman at al. (2010), Figure 2. The structure is gently dipping to the east, truncated by a pinch-out line to the west, Figure 3. The anticline was a result of tectonic activity during the Upper Cretaceous Syrian Arc folding system that created the symmetrical Heletz anticline.

The Heletz reservoir consists of three Lower Cretaceous sand layers; 'K', 'W' and 'A' separated by shales of various thicknesses deposited within sequences of repeated regressive – transgressive (marine – nearshore - coastal) depositional sequences, Amireh (1996), Eppelbaum and Katz, (2011). CO_2 Injection is into the reservoir layer 'W' where the reservoir sands have a maximum thickness of 21m in the South-East and pinch out to the West where the sands are replaced by shales. The caprock has a thickness increasing from 23 m in the North to 54 m in the South. δO^{18} values suggest a maximum burial temperature of around 60°C and a burial depth of around 1200 – 1400m, Levy, (1981).

Core samples have been provided from two wells (Figure 2), H-2 drilled and cored sometime between 1955 and 1960 and H-18 drilled and cored in 2013, Niemi at al. (2016).

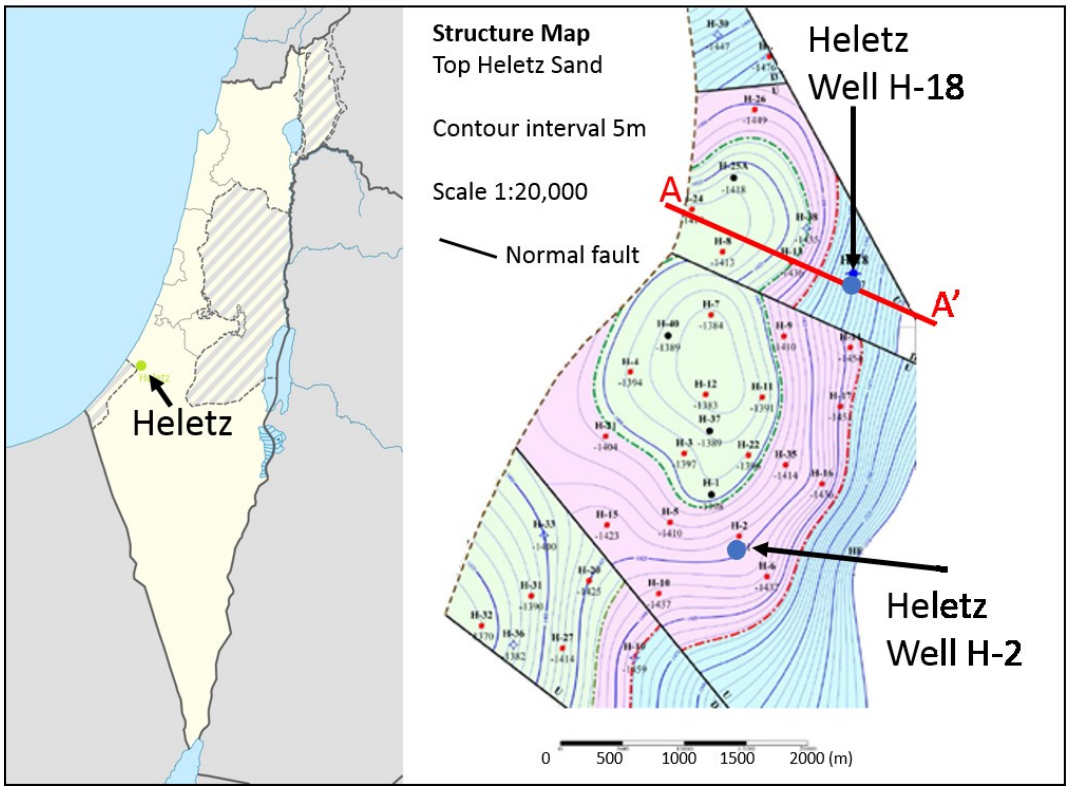

Figure 2 The Heletz location map and structure (from Shtivelman at al. 2010)

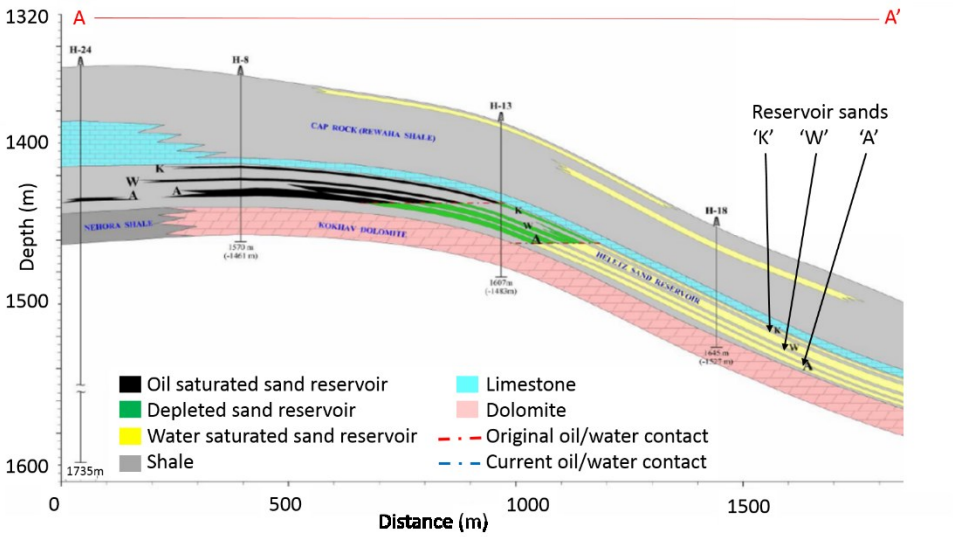

Figure 3 Heletz reservoir cross section (from Shtivelman at al. 2010)

2 Heletz mineralogy methods and results

Seven Heletz caprock samples and two Heletz reservoir sandstone were available for mineralogical and experimental testing from wells H-2 and the newly drilled Well H-18 (Figure 2). Their depths and images are presented in Table 1 and Figure 4.

Table 1 Heletz sample nomenclature, depth and year drilled and cored

Sample name	Depth (m)	Year drilled and cored
Heletz H-18 (sample A)	1596.00	2013
Heletz H-18 (sample B)	1596.04	2013
Heletz H-18 (sample C)	1596.08	2013
Heletz H-18 (sample D)	1596.39	2013
Heletz H-18 (sample E)	1596.43	2013
Heletz H-18 (sample F)	1596.47	2013
Heletz H-2 (sample A)	Unknown but higher up the anticline and shallower than the H-18 deposits	Between 1955 and 1960
Heletz H-18 Sandstone 1	1634.00	2013
Heletz H-18 Sandstone 1	1634.00	2013

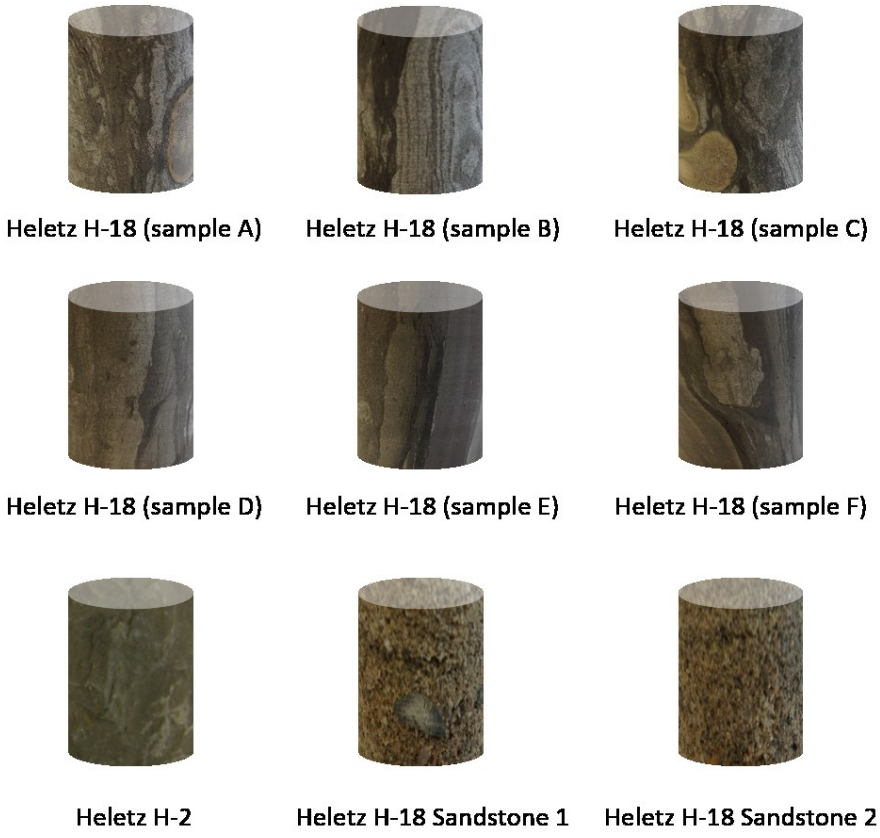

Figure 4 Heletz caprock samples from Well H-18 and H-2, plus two reservoir sandstones from Well H-18.

The mineralogy of the Heletz samples was determined using X-Ray diffraction (XRD) in a Bruker D8 Advance with Sol-X Energy Dispersive detector, in conjunction with the Bruker Diffrac.EVA software utilising the currently available International Centre for Diffraction Data (ICDD) database. Quantitative analysis is available using the TOPAS 3.0 Rietveld analysis software. The rock sample was placed in a tungsten carbide crushing mill to create chips. The chips were then placed in a Tema orbital mill for 2-3 minutes to create the powdered sample. For the sandstone, it was necessary to hand grind the powder to obtain the desired grain size of 50µm. The powdered samples were then placed in a glass mount making sure the surface was completely flat before being placed in the XRD instrument for quantitative Rietveld analysis. Extra care was taken not to over flatten the top layer of powder to ensure a fresh grain surface for analysis. Five different aliquots of each powdered sample were analysed which involved remounting the samples to get a fresh alignment of minerals on the top surface. This was in order to increase the precision of the results and to get an indication of the sampling and instrumental errors involved.

Table 2 and Figure 5 present the XRD mineralogy results for all the Heletz caprock samples. It can be seen that for all of the H-18 Heletz caprock samples the dominant mineral is K-feldspar (average 41wt%) followed by plagioclase feldspar (average 15wt%), kaolinite (average 11wt%), muscovite (average 8wt%) and illite (average 7% wt%) with minor chlorite and calcite (both average of 5wt%), quartz (average 3wt%), ankerite and pyrite (both with average 2wt%) and trace dolomite and siderite. Heletz well H-2 is dominated by kaolinite (23wt%) followed by K-feldspar (17wt%), illite and

muscovite(both with 11wt%), quartz (9wt%), plagioclase and chlorite (6wt%), calcite (5wt%) and pyrite (2.5wt%) with minor siderite, dolomite and ankerite.

There is a degree of variability of mineral distribution between the caprock samples. Figure 6 is a box and whisper plot for the caprock sample mineralogy and shows that in particular there is variability within the aluminosilicates followed by the clays and calcite; all of the minerals most likely to react with the CO_2 saturated brine.

Looking in more detail at the difference between the H-2 and H-18 caprocks, it can be identified that the H-2 caprock has a higher quartz, illite and kaolinite composition and a lower plagioclase feldspar and potassium feldspar composition than H-18 caprocks. The lower feldspar and increased kaolinite combined with the increased illite and quartz contents of the H-2 caprocks may indicate that the H-2 caprocks have undergone more diagenetic alteration than the H-18 caprocks.

Table 2 Heletz H-18 and H-2 caprock XRD mineralogy results

Group	Mineral	Heletz H-18 (Sample A)	Heletz H-18 (Sample B)	Heletz H-18 (Sample C)	Heletz H-18 (Sample D)	Heletz H-18 (Sample E)	Heletz H-18 (Sample F)	Heletz H-2 (Sample A)
Silicates	Quartz	1.6	1.9	5.1	3.6	3.2	0.3	9
	Plagioclase Feldspar	11.2	12.2	12.6	17.8	17.4	16.1	6.2
	K-feldspar	35.7	33.8	29.0	54.8	48.2	46.1	17.1
Clays	Illite	5.1	11.6	10.0	2.5	4.4	6.7	11.4
	Kaolinite	8.7	14.3	12.2	7.3	11.6	12.1	23.3
Mica	Muscovite	8.9	10.9	10.0	2.1	4.9	9.9	11.6
Chlorite	Chlorite	3.2	5.3	6.1	2.3	6.7	4.9	6.8
Carbonates	Calcite	19.1	3.6	4.9	0.6	0.0	0.0	4.9
	Dolomite	0.3	2.0	1.9	1.6	0.0	0.0	1.5
	Siderite	0.4	0.4	0.1	0.2	0.3	0.6	1.59
	Ankerite	2.3	1.7	2.4	3.3	1.1	0.8	0.1
Sulphides	Pyrite	2.2	2.3	3.0	3.2	1.4	2.2	2.45
	Gypsum	1.4	0.0	2.6	0.6	0.7	0.3	1.81

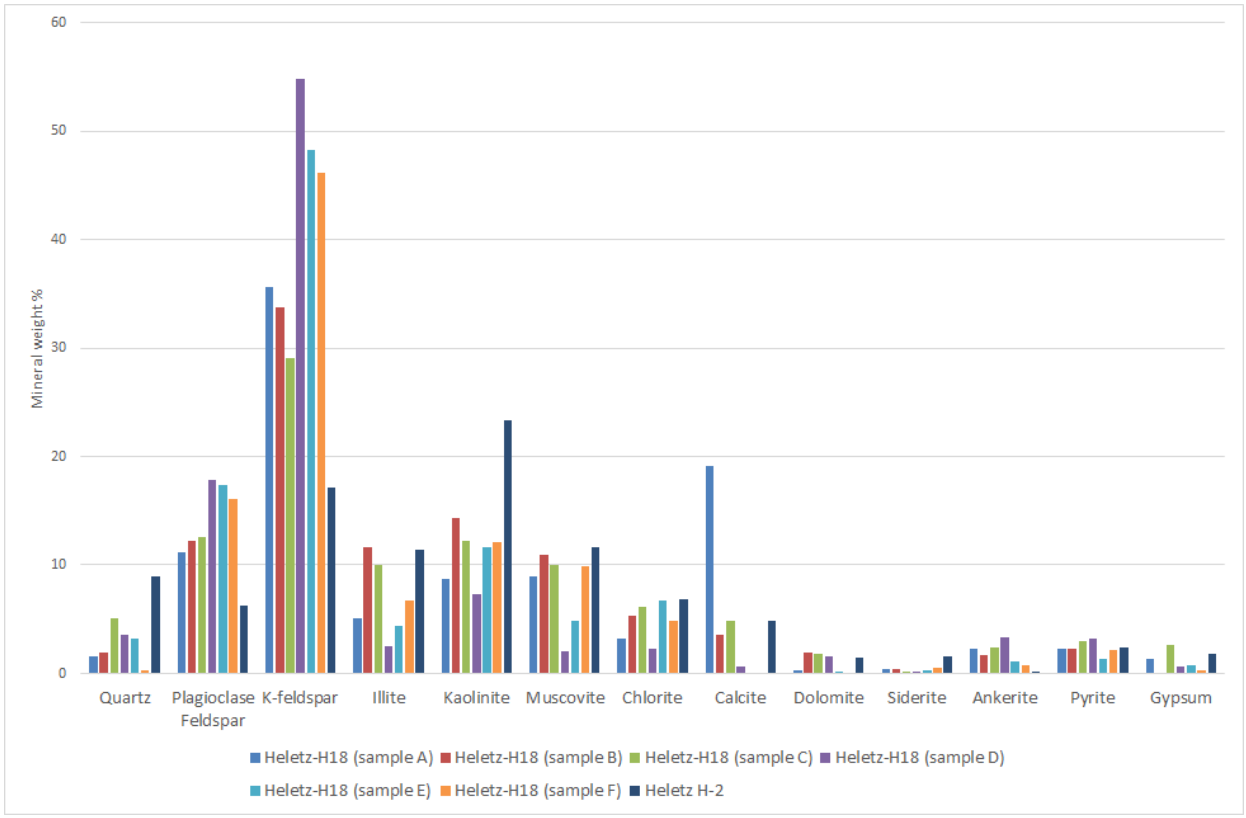

Figure 5 Heletz H-18 and H-2 caprock XRD mineralogy results

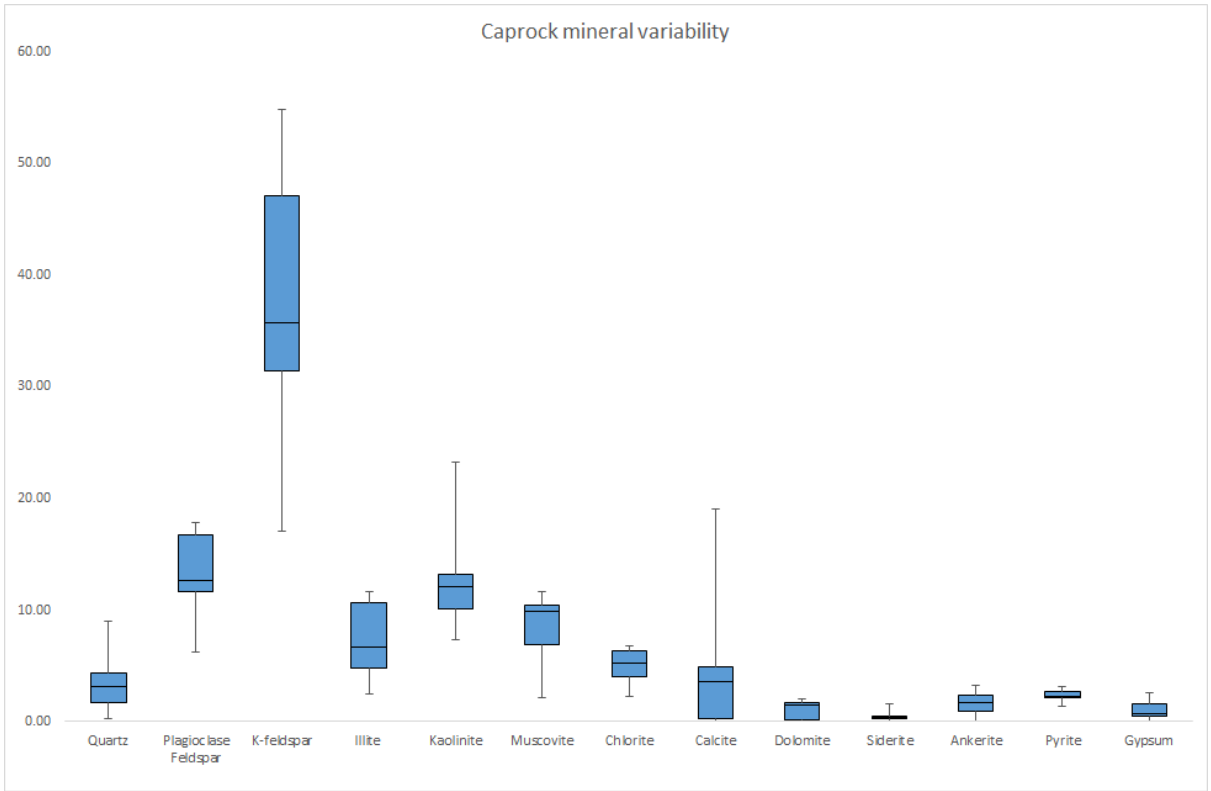

Figure 6 Box and whisper plot showing the variability within the mineralogy of the Heletz caprock samples

Table 3 and Figure 7 present the XRD mineralogy results for the reservoir sandstone samples. These Heletz sand 'W' reservoir sandstones are primarily quartz (average 70wt%) and K-feldspar (average 12wt%) with plagioclase feldspar (average 4wt%) kaolinite (average 3.2wt%), illite (average 2.6wt%) and pyrite (average 2wt%) with minor ankerite, chlorite, muscovite, dolomite, siderite and calcite. There is very little variability within the mineralogy between samples, Figure 8, with only quartz and kaolinite showing limited variability.

Table 3 Heletz H-18 sandstone XRD mineralogy results

Group	Mineral	Heletz H-18 (Sandstone 1)	Heletz H-18 (Sandstone 2)
Silicates	Quartz	73.4	66.0
	Plagioclase Feldspar	3.4	4.4
	K-feldspar	11.1	12.9
Clays	Illite	2.0	3.3
	Kaolinite	1.3	5.0
Mica	Muscovite	1.1	1.3
Chlorite	Chlorite	0.7	2.0
Carbonates	Calcite	0.0	0.1
	Dolomite	1.8	0.3
	Siderite	1.0	0.5
	Ankerite	2.1	1.5
Sulphides	Pyrite	1.8	2.3
	Gypsum	0.4	0.4

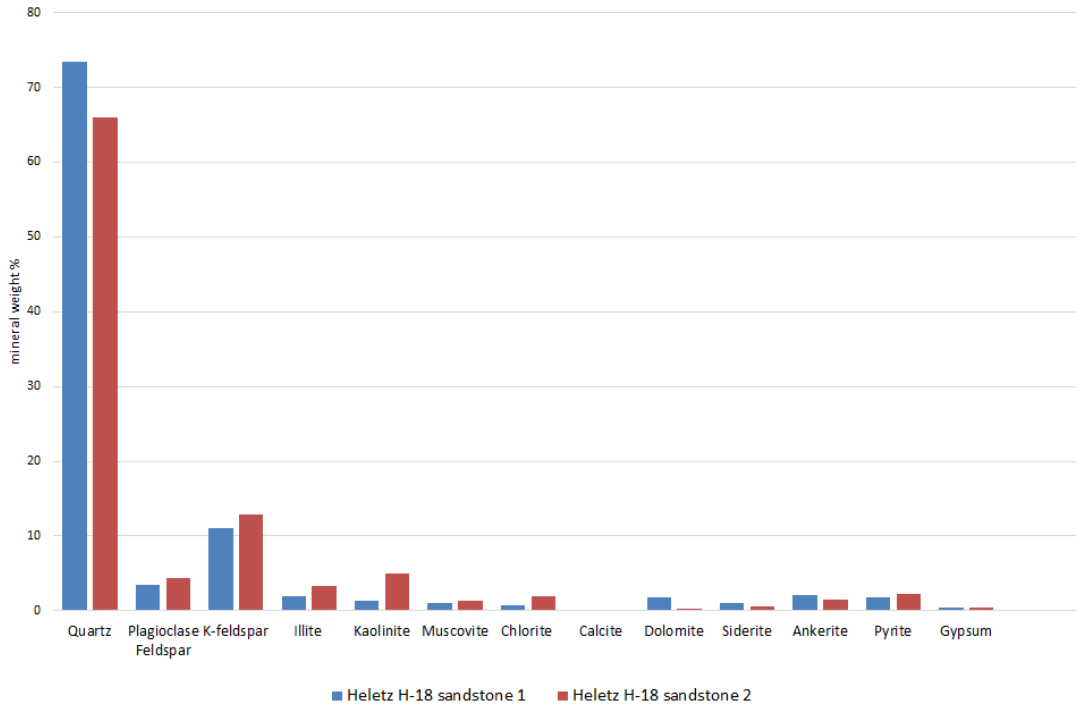

Figure 7 Heletz H-18 sandstone XRD mineralogy results

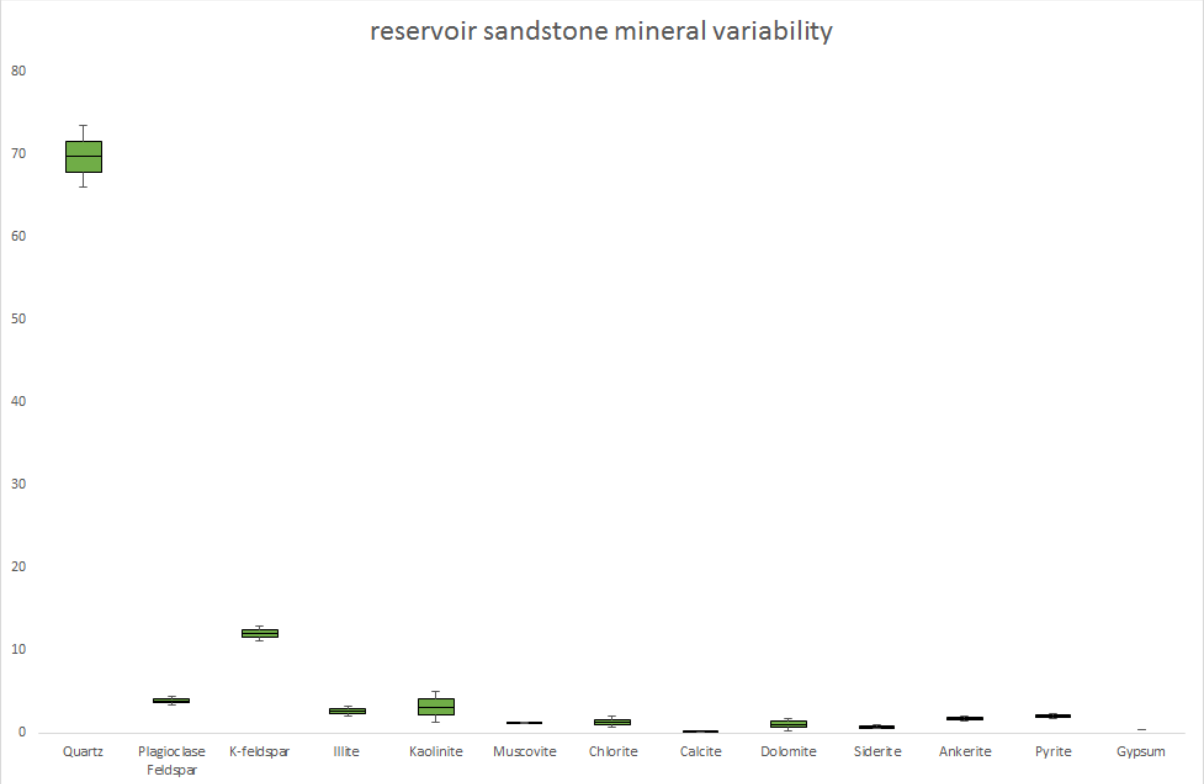

Figure 8 Box and whisper plot showing the variability within the mineralogy of the Heletz reservoir sandstone samples

3 Experimental methodology

Samples of Heletz caprock and sandstone were exposed to CO_2 saturated brine in simple "cook and look" bench experiments for 3 months that were designed to identify if there was any immediate mineral reactivity within the caprock or reservoir sandstone on exposure to CO_2 that could serve to alter permeability which may raise concerns during well completion and initial injection of CO_2 at Heletz.

The experimental equipment comprises a 3 arm conical flask, Ludwig condenser, heating mantle, thermometer and CO_2 inlet, Figure 9 which facilitated the exposure of Heletz rocks to CO_2 saturated brine under conditions of reservoir temperature and salinity. The experimental conditions were:

- Conical 3-arm flask containing 100g of 5mm diameter rock chip samples.
- Temperature of 55°C. Satrinsky (1974) indicates a maximum temperature of 50-60°C at 1500-1800m for the Heletz reservoir.
- Brine of 35,000ppm NaCl. The logging report for Heletz well H-38 provided a salinity defined by DST of 35,000 – 40,000ppm at 1050m depth and of 22,113ppm Cl at 1555m.
- Ambient pressure.
- Gas phase CO_2 is continually bubbled through the brine at around 0.5ml/min to ensure a consistently CO_2 saturated brine.
- The experiment is static, with no stirring or agitation of the rock chip samples.

- Two identical experimental set-ups are run in tandem. One is run without CO_2 as a reference to identify the changes brought about by reactivity with brine so that any changes due to CO_2 can be identified.
- The experiments were run for 3 months.

There were two analytical strategies used during the experiments:

- Before the experiment half of the rock chips to be used in each of flasks were taken for bulk XRD analysis to obtain the bulk mineralogy before the experiment. The other half of the chips were added to each of the flasks for the bench experiments. At the end of the experiment the remaining rock chips from each of the flasks were taken for bulk XRD analysis to identify if there was any bulk mineralogical changes after 3 months.
- As there was an absence of fluid analysis equipment available at the time of the experimental program, Scanning Electron Microscope (SEM) analysis of the surfaces of the rock chips was undertaken for the duration of the experiments. A single Heletz caprock chip was removed from both of the flasks every week for SEM analysis to identify if there are any distinct mineralogical changes within the Heletz caprock and reservoir rock on exposure to CO_2.

The sampling of different chips to identify any change in the rocks due to exposure to CO_2 will be influenced by the variability of the rock samples as highlighted in Figures 6 and 8. This is due to the compositional variability / heterogeneity within the rock samples themselves. This was minimised by selecting the most homogeneous rock from which to take the chips. The bulk XRD analysis at the beginning and end of the experiments will also provide average end member mineralogy which will not be so vulnerable to sample variability sensitivity.

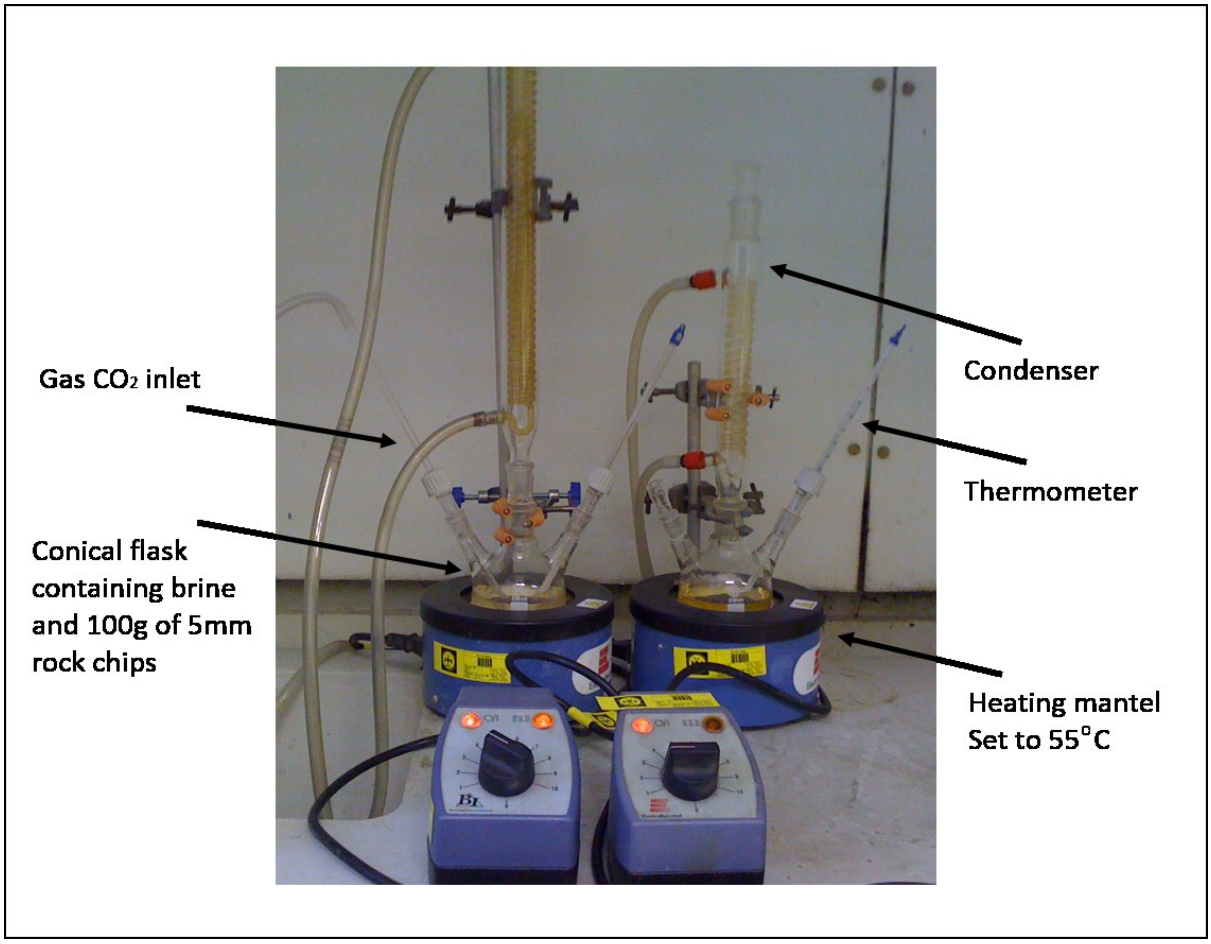

Figure 9 CO_2 saturated brine bench experiment equipment

4 Results and discussion

Considering the mineralogy of the Heletz caprock and reservoir rocks, Tables 2 and 3, some of the reactivity dissolution markers include, Velde, (1995):

- A decrease in calcite (or dolomite $CaMg(CO_3)_2$) as a result of carbonate reactivity: $CaCO_3$ (calcite) + H+ ⇌ Ca^{2+} + HCO_3^-
- A decrease in k-feldspar and increase in illite as a result of the digenetic breakdown of the aluminosilicate K-feldspar: $3KAlSi_3O_8$ (*K-Feldspar*) + $2H^+$ + $12H_2O$ ⇌ $2K^+$ + $6Si(OH)_4^0$ + $KAl_3Si_3O_{10}(OH)_2$ (*illite*)
- A decrease in Kaolinite and increase in illite as a result of the reactivity of kaolinite: kaolinite + cation (K^+) ⇌ illite + quartz + water.

4.1 Heletz H-2 caprock / CO_2 saturated brine reactivity

Table 4 and Figure 10 present the bulk XRD mineralogy of the Heletz H-2 shale caprock before testing, after the three months of exposure to brine only and CO_2 saturated brine at 55°C.

Table 4 Heletz H-2 XRD results before and after the CO_2 exposure experiments

Group	Mineral	Heletz H-2 (before testing)	Heletz H-2 (brine and temperature only)	Heletz H-2 (brine, temperature and CO_2)
Silicates	Quartz	9.0	6.0	1.5
	Plagioclase Feldspar	6.2	8.4	4.5
	K-feldspar	17.1	15.3	16.3
Clays	Illite	11.4	11.2	23.0
	Kaolinite	23.3	24	22.7
Mica	Muscovite	11.6	15.1	9.2
Chlorite	Chlorite	6.8	9.0	10.3
Carbonates	Calcite	4.9	4.6	3.5
	Dolomite	1.5	0.0	1.2
	Siderite	1.6	1.6	1.6
	Ankerite	0.1	1.0	0.0
Sulphides	Pyrite	2.4	1.1	0.2
	Gypsum	1.8	2.4	6.0

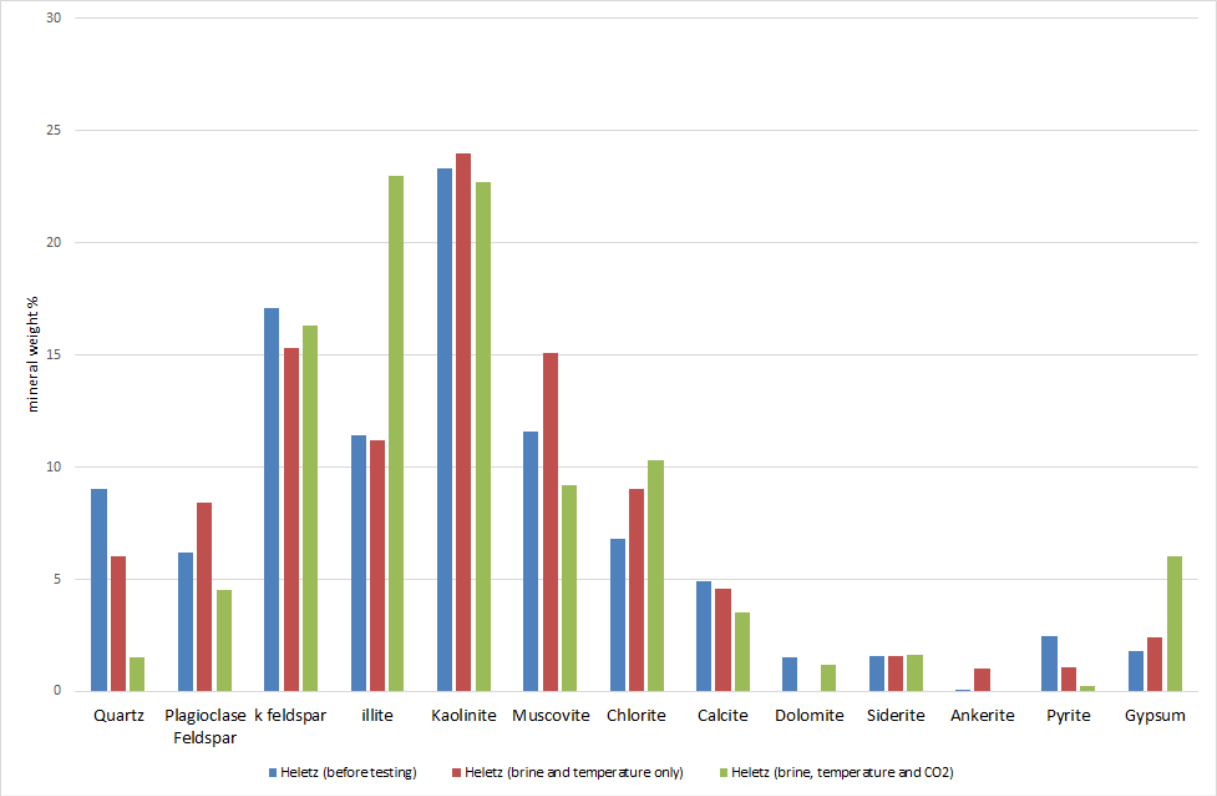

Figure 10 Heletz H-2 mineralogy before and after CO_2 exposure

4.1.1 Reactivity of the Heletz H-2 caprock carbonate minerals

The bulk XRD analysis indicated that there was a slight decrease in the carbonate minerals within the Heletz H-2 caprock on exposure to CO_2 saturated brine over 3 months, with calcite reducing from 4.9 to 3.5 wt% and dolomite reducing from 1.5 to 1.2 wt%. SEM investigations revealed a lack of calcite minerals within the samples exposed to CO_2 for 3 months which had been observed at the beginning of the experiment, Figure 11.

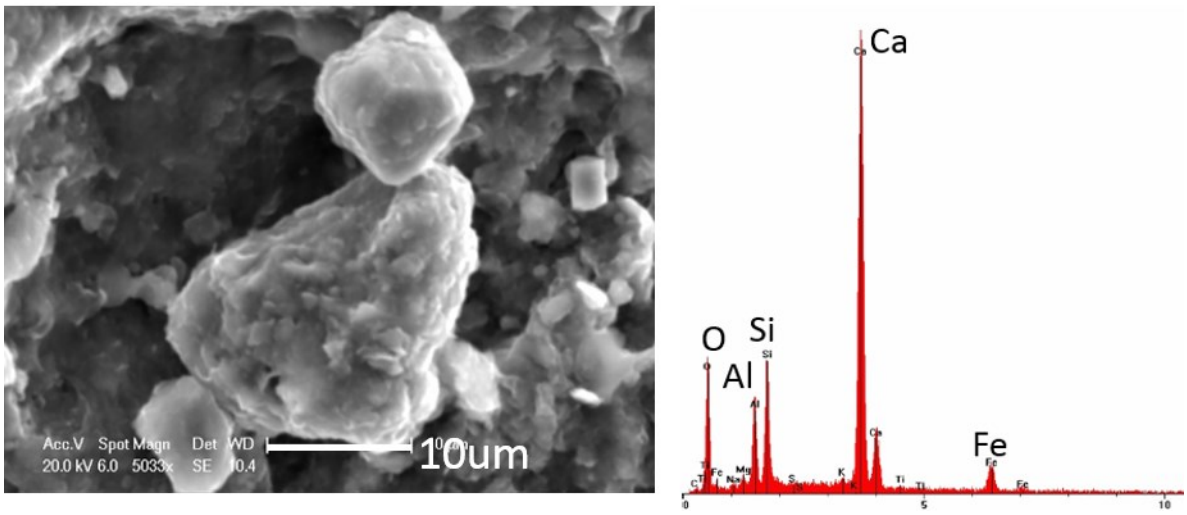

Figure 11 Calcite minerals identified at the beginning of the experiment but absent after 3 months exposure to CO_2 saturated brine.

There is a high percentage of calcite in one of the Heletz H-18 caprocks (Sample A, Table 2) with all the other samples having low amounts of calcite (average of 2.3wt%), therefore permeability reduction due to carbonate dissolution is not likely to be a risk to the integrity of the Heletz caprock during drilling and initial injection.

4.1.2 Reactivity of the Heletz H-2 caprock alumina-silicate / clay minerals

The bulk XRD analysis indicated that there was an observed increase in illite in the samples exposed to brine and CO_2 for 3 months, from 11.4 wt% to 23wt%, which could be a result of the breakdown of K-feldspar to illite or the breakdown of kaolinite to illite. Both k-feldspar and kaolinite do show a decrease in weight percentage from 17.1 to 16.3 and 23.3 to 22.7 respectively, however this does not balance with the amount of illite increase. The SEM investigations during the experiments did not reveal any wispy authigenic illite crystals on the chip surfaces that would indicate the diagenetic breakdown of K-feldspar or kaolinite to illite and the surfaces become weathered and amorphous, Figure 12. In addition looking at the natural variability between samples of Heletz caprock of k-feldspar, kaolinite and illite, Table 2 and Figure 6, the analysis reveals a variability of weight percentage of K-feldspar to be between 17.1% and 54.8%, kaolinite to be between 7.3% and 23.3%, and illite between 2.5% to 11.6%, for the Heletz caprock, which confirms a reasonable degree of variability of k-feldspar, kaolinite and Illite distribution within the Heletz caprock samples, however it should not be discounted that there is the possibility of a net illite precipitations within the caprock and an associated decrease in permeability and change in caprock properties.

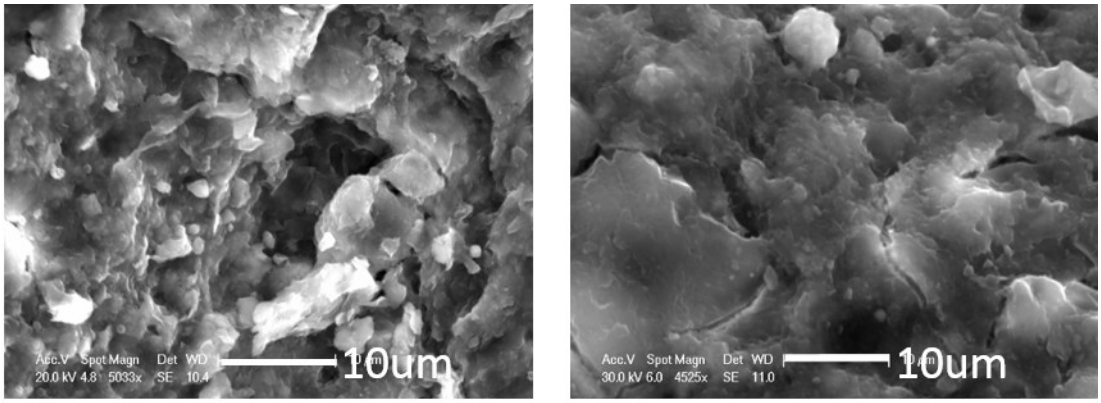

Figure 12 SEM of caprock matrix surface before and after CO_2 exposure

4.1.3 Reactivity of the Heletz H-2 caprock quartz.

The bulk XRD analysis indicated that these was an observed decrease in quartz in the caprock samples exposed to brine and CO_2 for 3 months from 9wt% to 1.5wt%. The timescales and experimental conditions of these experiments rule out the alteration of quartz and the difference is most likely due to the variability within the sample. Figure 6 and Table 2 shows the weight percentage of quartz within the Heletz caprock samples ranges from 0.3% to 9%, which confirms this high degree of variability of quartz distribution within the Heletz caprock samples. SEM investigations, Figure 13, show little evidence for any surface changes on the quartz crystals, with no obvious changes in the angles of the edges or in pits on exposure to CO_2.

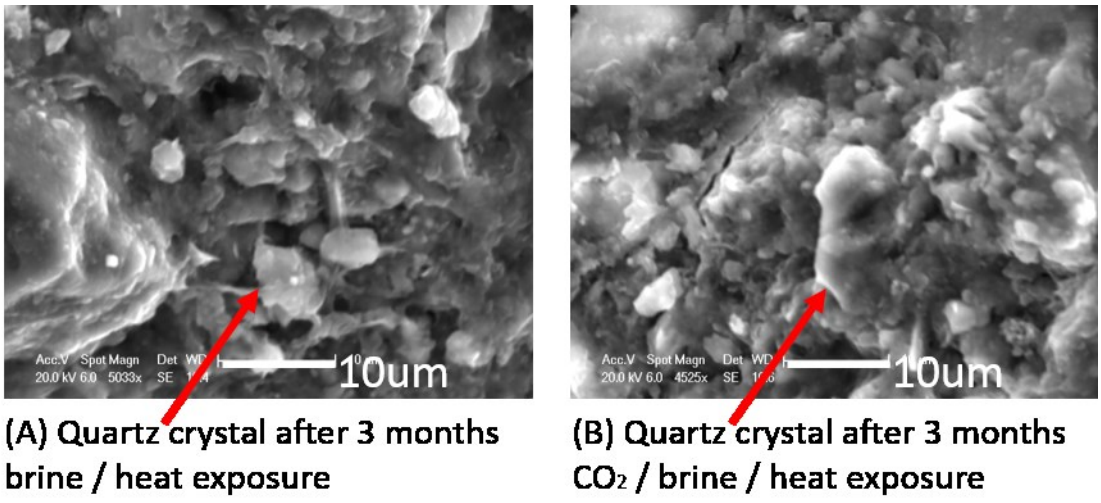

Figure 13 SEM investigation into potential quartz reactivity

4.2 Heletz H-18 reservoir sandstone CO_2 reactivity

The Heletz H-18 sandstone is relatively soft and although consolidated, there were indications that it would not withstand the bench experiments. So prior to breaking the Heletz H-18 (sandstone 2) into chips it was placed in a beaker of Heletz brine and the sample completely disintegrated into its component parts, Figure 14.

This meant that the sandstone samples were not tested in the bench experiments and the disintegration findings were directly communicated to the Heletz drilling team as a potential risk during completion and injection. To a certain degree this was observed in the field. Well H-18 was cemented and after cementation the wells were flushed with fresh water and the well perforated. A few months later a pump test was performed and the test revealed that the well was clogged due to mixing between the freshwater in the borehole and the formation water resulting in clay swelling, Fe hydroxides and other chemical processes, Luquot et al., (2016). Injectivity was restored by injecting KCL into the well and performing 20 swab-suctions.

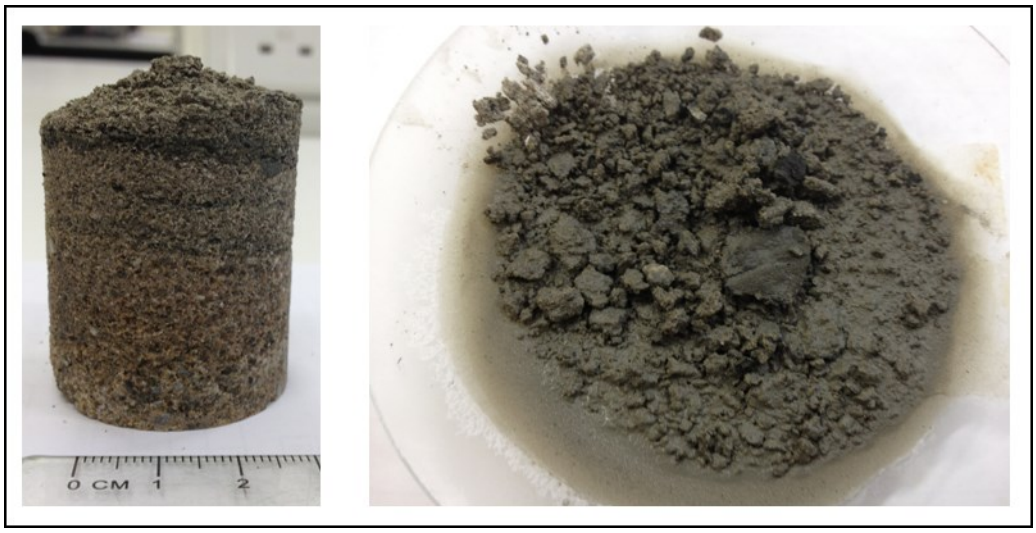

Figure 14 Heletz H-18 sandstone before and after saturation in synthetic Heletz brine.

4.3 Further discussions

The "cook and look" experiments were undertaken with at ambient pressure and elevated temperature where the CO_2 is in its gas phase. The Heletz storage site depth and temperature means that the CO_2 will be in its supercritical state. Previous work on the interaction of $scCO_2$ and fractured caprock by the author, Edlmann et al., (2013) indicated little or no reactivity and as such the findings from these investigations will hold under the Heletz site storage conditions.

5 Conclusions

It can be seen that for all of the H-18 Heletz caprock samples the dominant mineral is K-feldspar followed by plagioclase feldspar, kaolinite, muscovite and illite with minor chlorite and calcite, quartz, ankerite and pyrite and trace dolomite and siderite. Heletz well H-2 is dominated by kaolinite followed by K-feldspar illite and muscovite, quartz, plagioclase and chlorite, calcite and pyrite with minor siderite, dolomite and ankerite. The H-2 caprock has a higher quartz, illite and kaolinite composition and a lower plagioclase feldspar and potassium feldspar composition than H-18 caprocks. The lower feldspar and increased kaolinite combined with the increased illite and quartz contents of the H-2 caprocks may indicate that the H-2 caprocks have undergone more diagenetic alteration than the H-18 caprocks.

While there are some minor observed changes in the mineralogy on exposure to CO_2 saturated brine these observations were within the natural variability between the Heletz caprock samples and as such the "cook and look" bench experiments revealed that there is no significant mineral reactivity

that would alter permeability in the Heletz caprock that could cause concerns during well completion and initial injection of CO_2 at Heletz.

The Heletz H-18 sandstone became completely unconsolidated when exposed to Heletz brine and this reactivity was also observed in the field. During completion of Well H-18 loss of injectivity occurred clay swelling, Fe hydroxides and other chemical processes, which was restored by injecting KCL into the well and performing 20 swab-suctions.

6 Acknowledgements

The research leading to these results has received funding from the European Community's Seventh framework Programme FP7/2007-2013 under the grant agreement No. 227286 MUSTANG - A Multiple Space and Time scale Approach for the quaNtification of deep saline formations for CO_2 storaGe and from the Scottish Funding Council for the Joint Research Institute with the Heriot-Watt University which is part of the Edinburgh Research Partnership in Engineering and Mathematics (ERPem).

7 References

Amann, A., Waschbüsch, M., Bertier, P., Busch, A., Kroossa, B.M., Littke R., 2011. Sealing rock characteristics under the influence of CO_2, Energy Procedia. 4, 5170–5177.

Amireh B.S. 1997. Sedimentology and palaeogeography of the regressive-transgressive Kurnub Group (Early Cretaceous) of Jordan Sedimentary Geology 112, p. 69-88.

Bachu, S. 2003. Screening and ranking sedimentary basins for sequestration of CO_2 in geological media in response to climate change. Environmental Geology, 44**,** pp 277−289.

Benson S, Cook P, Anderson J, Bachu S, Nimir HB, Basu B, Bradshaw J, Deguchi G, Gale J, Goerne GV, Heidug W, Holloway S, Kamal R, Keith D, Lloyd P, Rocha P, Senior B, Thomson J, Torp T, Wildenborg T, Wilson M, Zarlenga F, Zhou D. 2005. Underground geological storage. In: Metz B, Davidson O, Coninck HD, Loos M, Meyer L (eds) Carbon dioxide capture and storage: special report of the Intergovernmental Panel on Climate Change. Cambridge University Press, New York, pp 195–276

Busch, A., Amann, A., Bertier, P., Waschbusch, M. and Kroos, B.M., 2010. The Significance of Caprock Sealing Integrity for CO_2 Storage. SPE 139588.

Czernichowski-Lauriol, I., Rochelle, C., Gaus I., Azaroual, M., Pearce, J., and Durst P. 2006. Geochemical Interactions between CO_2, Pore-Waters and Reservoir Rocks Lessons learned from laboratory experiments, field studies and computer simulations. In. Lombardi, S. et al. (eds.), Advances in the Geological Storage of Carbon Dioxide, 157–174. 2006 Springer.

Class, H. (Ed.) 2009. A benchmark study on problems related to CO_2 storage in geologic formations, Summary and discussion of the results Comput Geosci. 13, 409–434.

DePaolo, D.J., Cole, D.R. 2013 Geochemistry of geologic carbon sequestration: An overview, Reviews in Mineralogy and Geochemistry. Volume 77, Issue 1, Pages 1-14.

Duan, Z. and R. Sun, 2003. An improved model calculating CO_2 solubility in pure water and aqueous NaCl solutions from 273 to 533 K and from 0 to 2000 bar, Chem. Geol., 193, p. 257-271.

Duan, Z. and R. Sun Zhu C. and Chou I-M. 2006 An improved model for the calculation of CO_2 solubility in aqueous solutions containing Na^+, K^+, Ca^{2+}, Mg^{2+}, Cl^-, and SO_4 Marine Chemistry 98. P. 131–139.

Edlmann, K., Haszeldine S. and McDermott, C. I., 2013. Experimental investigation into the sealing capability of naturally fractured shale caprocks to supercritical carbon dioxide flow. Environmental Earth Science 20, pp 3393-3409

Eppelbaum, L. and Katz, Y. 2011 Tectonic-Geophysical Mapping of Israel and the Eastern Mediterranean: Implications for Hydrocarbon Prospecting. doi:10.4236/pos.2011.21004. Published Online February 2011 (http://www.SciRP.org/journal/pos).

Fischer, S., Liebscher, A. and Wandrey, M., 2010. CO_2–brine–rock interaction: First results of long-term exposure experiments at insitu P–T conditions of the Ketzin CO_2 reservoir. Chemie der Erde 70, S3, 155–164.

Fitts B.J.P. and C.A. Peters C.A., Caprock Fracture Dissolution and CO_2 Leakage, 2013. In: Geochemistry of Geologic CO_2 Sequestration (Eds: DJ DePaolo, DR Cole, A Navrotsky, IC Bourg), Reviews in Mineralogy & Geochemistry Vol 77: 459 – 479.

Gaus, I. 2010. Role and impact of CO_2–rock interactions during CO_2 storage in sedimentary rocks, International Journal of Greenhouse Gas Control, 4, 73–89.

Griffith C.A., Dzombak D.A., Lowry G.V. 2011. Physical and chemical characteristics of potential seal strata in regions considered for demonstrating geological saline CO_2 sequestration. Environ Earth Sci 64(4):925-948

IEAGHG 2011. Caprock systems for CO_2 geological storage, Report 2011/01, May 2011.

Kampman, N., Bickle, M., Wigley, M. and Dubacq, B. 2014. Fluid flow and CO_2–fluid–mineral interactions during CO_2-storage in sedimentary basins Chemical Geology 369 (2014) 22–50.

Ketzer, J.M., Iglesias, R., Einloft, S., Dullius, J., Ligabue, R. and De Lima, V. 2009. Water–rock–CO_2 interactions in saline aquifers aimed for carbon dioxide storage: Experimental and numerical modelling studies of the Rio Bonito Formation (Permian), southern Brazil. Applied Geochemistry. 24, 760–767.

Knauss, K.G., Johnson, J.W., And Steefel, C.I., 2005, Evaluation of the impact of CO_2, co-contaminant gas, aqueous fluid and reservoir rock interactions on the geologic sequestration of CO_2: Chemical Geology, v. 217, p. 339–350.

Koide, H., Tazaki Y., Noguchi Y., Nakayama S., Iijima M., Ito K. and Shindo Y. 1992. Subterranean containment and long term storage of carbon dioxide in unused aquifers and in depleted natural gas reservoirs. Energy Convers. Manag. 33 (5-8), 619-626.

Landrot G., Ajo-Franklin j., Cabrini, S., Yang, L. and Steefel C.I. 2012. Measurement of accessible relative surface area in a sandstone, with application to CO_2 mineralisation. Chem Geol 318-319:113-125.

Li, Z., Dong, M., Li, Z., Huang, S., Qing, H., Nickel, E., 2005. Gas breakthrough pressure for hydrocarbon reservoir seal rocks: implications for the security of long-term CO_2 storage in the Weyburn field. Geofluids. 5: p. 326-334.

Li, Z., Dong, M., Li, S., Huang, S., 2006. CO_2 sequestration in depleted oil and gas reservoirs—caprock characterization and storage capacity. Energy Conversion and Management. 47: p. 1372–1382.

Loring, J.S., Schaef, H.T., Thompson, C.J., Turcu, R.V., Miller, Q.R., et al., 2013. Clay Hydration/dehydration in Dry to Water-saturated Supercritical CO_2: Implications for Caprock Integrity, Energy Procedia, Volume 37, 2013, Pages 5443-5448.

Luquot, L., Gouze, P., Carrera, J., Niemi, A. and Bensabat, J. 2016. Laboratory experiment of CO_2-rich brine percolation experiments through Heletz samples (Israel): Role of the flow rate and brine composition. International Journal of Greenhouse Gas Control, This issue.

Michael K., Golab A., Shulakova V., Ennis-King J., Allinson G., Sharma S. and Aiken T. 2010. Geological storage of CO_2 in saline aquifers-A review of the experience from existing storage operations. Int J Greenhouse Gas Control 4(4):659-667.

Niemi, A., Bensabat, J., Fagerlund, F., Sauter, M., Ghergut, J., Licha, T., Fierz, T. Wiegand, G., Rasmusson, M., Rasmusson, K., Shtivelman, V. Gendler, M. and MUSTANG Partners. 2012. Small scale injection into a deep geological formation at Heletz, Israel. Energy Procedia Volume: 23 Pages: 504-511.

Niemi, A., Bensabat, J., et al. 2016 Overview of the Heletz site, its characterization and data analysis for CO_2 geological storage. International Journal of Greenhouse Gas Control, This issue.

Nogues, J.P., Fitts J.P., Celia M.A. and Peters C.A., 2013 Permeability evolution due to dissolution and precipitation of carbonates using reactive transport modeling in pore networks. Water Resources Research, Vol. 49, 6006–6021, doi:10.1002/wrcr.20486.

Rochelle, C. A., Czernichowski-Lauriol, I. and Milodowski, A. E. 2004. The impact of chemical reactions on CO_2 storage in geological formations: a brief review: Geological Society of London, Special Publications, 233, 87– 106.

Rosenbauer, R.J., Koksalan, T., Palandri, J.L. 2005 Experimental investigation of CO_2-brine-rock interactions at elevated temperature and pressure: Implications for CO_2 sequestration in deep saline aquifers, Fuel Processing Technology, 86, 1581-1597

Rosenqvist, J.; Kilpatrick, A. D.; Yardley. Rochelle, Christopher A. 2014. Dissolution of K-feldspar at CO_2 -saturated conditions Geophysical Research Abstracts. Vol. 16, EGU2014-10909, 2014 EGU General Assembly 2014.

Satrinsky A. 1974. Relationship between Ca-chloride brines and sedimentary rocks in Israel. PhD dissertation, Hebrew University. Jerusalem.

Shtivelman. V., Gendler, M. and Goldberg I., 2010. 3D structure of Heletz site in MUSTANG Deliverable D022.

UK Met Office Data, 2010 - www.metoffice.gov.uk/climatechange

Velde B. 1995. Origin and Mineralogy of Clays. Springer Verlag.